2017 International Symposium on Nonlinear Theory and Its Applications,
NOLTA2017, Cancun, Mexico, December 4-7, 2017

Stability analysis of amplitude death in delayed coupled oscillators on a cubic graph with three different connection delays

Takahiro KIKUCHI† and Yoshiki SUGITANI†

†Graduate School of Science and Engineering, Ibaraki University
4–12–1, Nakanarusawa, Hitachi, Ibaraki, 316–8511 Japan
Email: yoshiki.sugitani.0301@vc.ibaraki.ac.jp

Abstract—The present study investigates the stability of amplitude death in a delayed coupled oscillator network on a cubic graph. The oscillator network on the cubic graph is constructed using the Cartesian product of three sub-networks, with path graph topology comprising two nodes. As the sub-networks have different connection delays, the connection delays of the oscillator network are not identical. Although such an oscillator network is difficult to be analyzed, the property of the Cartesian product allows the simple analysis of stability. The analytical results are confirmed via numerical simulations.

1. Introduction

Amplitude death, which is the stabilization of an unstable equilibrium point in coupled oscillators[1], is induced by diffusive interactions between oscillators [2]. It has been confirmed that amplitude death never occurs in diffusively coupled identical oscillators [3], [4]. However, in 1998 Reddy *et al.* found that a connection delay can cause amplitude death even in identical coupled oscillators [5], [6]. Amplitude death by delay has attracted considerable attention not only in the academic field but also in the field of engineering such as DC micro grids [7, 8]. Most of the previous studies on amplitude death assume that all connection delays between oscillators are identical in the entire network [9–15], even though there are many real networks with non-identical delays. This is because it is difficult to analyze the stability of amplitude death in networks with non-identical connection delays.

To investigate amplitude death in networks with non-identical connection delays, our previous study dealt with Cartesian product networks of two sub-networks, where each sub-network had different connection delays (see Fig. 1(a)) [16]. As a result, the Cartesian product network contained two different connection delays. As mentioned above, the stability of such network is difficult to be analyzed. However, the properties of the Cartesian product [17, 18] allow a simple analysis of stability. Our previous study revealed that there is a suitable difference between the two connection delays in the two sub-networks to induce amplitude death for the long connection delays. However, the networks analyzed in our previous study contained only two different connection delays.

In this study, we investigate amplitude death in a network on a cubic graph with three different connected delays (see Fig. 1(b)), based on our previous study [16]. The network on the cubic graph is constructed using the Cartesian product of three sub-networks, with path graph topology containing two nodes. The property of the Cartesian product enables the simple determination of the stability region. The analytical results are confirmed via numerical simulations.

2. Delayed coupled oscillators on a cubic graph

Let us consider delayed coupled oscillators on a cubic graph (see Fig. 1), which is constructed by the following three steps: (i) prepare three sub-networks $\mathcal{G}_1$, $\mathcal{G}_2$, and $\mathcal{G}_3$ with path graph topology with two nodes; (ii) construct a Cartesian product network $\mathcal{G}_1 \square \mathcal{G}_2$ from $\mathcal{G}_1$ and $\mathcal{G}_2$ (see Fig. 1(a)); (iii) construct a Cartesian product network $(\mathcal{G}_1 \square \mathcal{G}_2) \square \mathcal{G}_3$ from $\mathcal{G}_1 \square \mathcal{G}_2$ and $\mathcal{G}_3$ (see Fig. 1(b)). The connection delays in the Cartesian product network $(\mathcal{G}_1 \square \mathcal{G}_2) \square \mathcal{G}_3$ are not identical, as sub-networks $\mathcal{G}_1, \mathcal{G}_2$, and $\mathcal{G}_3$ has different connection delays τ_1, τ_2, and τ_3 (see Fig. 1(b)).

Note that the adjacency matrix of sub-networks $\mathcal{G}_1$, $\mathcal{G}_2$, and $\mathcal{G}_3$ is given by

$$\boldsymbol{A}_G = \begin{bmatrix} 0 & 1 \\ 1 & 0 \end{bmatrix}. \tag{1}$$

Hence, the adjacency matrices of $\mathcal{G}_1 \square \mathcal{G}_2$ and $(\mathcal{G}_1 \square \mathcal{G}_2) \square \mathcal{G}_3$ can be written as

$$\boldsymbol{A}_{\mathcal{G}_1 \square \mathcal{G}_2} = \boldsymbol{A}_G \otimes \boldsymbol{I}_2 + \boldsymbol{I}_2 \otimes \boldsymbol{A}_G, \tag{2}$$

$$\begin{aligned} \boldsymbol{A}_{(\mathcal{G}_1 \square \mathcal{G}_2) \square \mathcal{G}_3} &= \boldsymbol{A}_{\mathcal{G}_1 \square \mathcal{G}_2} \otimes \boldsymbol{I}_2 + \boldsymbol{I}_4 \otimes \boldsymbol{A}_G \\ &= \boldsymbol{A}_G \otimes \boldsymbol{I}_4 + \boldsymbol{I}_2 \otimes \boldsymbol{A}_G \otimes \boldsymbol{I}_2 + \boldsymbol{I}_4 \otimes \boldsymbol{A}_G, \end{aligned}$$

where symbol $\otimes$ and $\boldsymbol{I}_m$ denotes the Kronecker product and m-dimensional identity matrix, respectively.

[1] Amplitude and oscillation death are different phenomena [1].

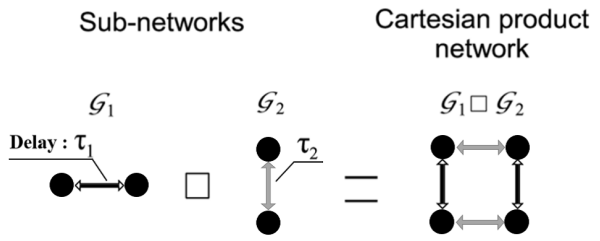

(a) Cartesian product network $\mathcal{G}_1\square\mathcal{G}_2$

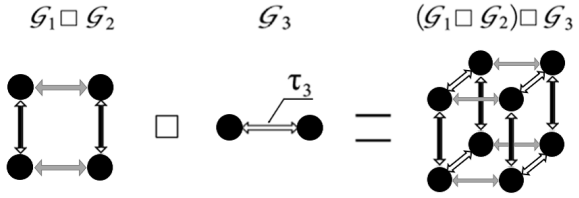

(b) Cartesian product network $(\mathcal{G}_1\square\mathcal{G}_2)\square\mathcal{G}_3$

Figure 1: Schematics of the delayed coupled oscillators on a cubic graph $(\mathcal{G}_1\square\mathcal{G}_2)\square\mathcal{G}_3$. Sub-networks $\mathcal{G}_1$, $\mathcal{G}_2$, and $\mathcal{G}_3$ contain connection delays τ_1, τ_2, and τ_3, respectively. All the sub-networks $\mathcal{G}_1$, $\mathcal{G}_2$, and $\mathcal{G}_3$ are path graphs with two nodes.

The present study considers the delay-coupled Stuart-Landau oscillators on the cubic graph,

$$\begin{aligned}\dot{Z}_i(t) = (\mu + j\omega - |Z_i(t)|^2)Z_i(t) \\ + u_i^{(1)}(t) + u_i^{(2)}(t) + u_i^{(3)}(t),\end{aligned} \quad (3)$$

where $i = 1, \ldots, 8$ and $Z_i(t) \in \mathbb{C}$ is the state variable of i-th oscillator. The imaginary unit is defined as $j := \sqrt{-1}$. Parameters $\mu > 0$ and $\omega > 0$ represent the instability and the natural frequency of the equilibrium point $Z_i^* = 0$, respectively. Each oscillator receives input signals $u_i^{(1)}(t), u_i^{(2)}(t)$, and $u_i^{(3)}(t)$ from subnetworks $\mathcal{G}_1, \mathcal{G}_2$, and $\mathcal{G}_3$, respectively:

$$\begin{aligned}u_i^{(1)}(t) &= k\Big\{\sum_{l=1}^{8} c_{i,l}^{(1)} Z_l(t-\tau_1) - Z_i(t)\Big\}, \\ u_i^{(2)}(t) &= k\Big\{\sum_{l=1}^{8} c_{i,l}^{(2)} Z_l(t-\tau_2) - Z_i(t)\Big\}, \\ u_i^{(3)}(t) &= k\Big\{\sum_{l=1}^{8} c_{i,l}^{(3)} Z_l(t-\tau_3) - Z_i(t)\Big\},\end{aligned} \quad (4)$$

where k is the coupling strength. τ_1, τ_2, and τ_3 denote the connection delays in subnetworks $\mathcal{G}_1, \mathcal{G}_2$, and $\mathcal{G}_3$, respectively. $c_{i,l}^{(1)}, c_{i,l}^{(2)}$, and $c_{i,l}^{(3)}$ represent the (i,l) element of adjacency matrices $\boldsymbol{A}_G \otimes \boldsymbol{I}_4$, $\boldsymbol{I}_2 \otimes \boldsymbol{A}_G \otimes \boldsymbol{I}_2$, and $\boldsymbol{I}_4 \otimes \boldsymbol{A}_G$ in Eq. (2), respectively: $c_{i,l}^{(1)} = 1$ and $(c_{i,l}^{(2)} = 1, c_{i,l}^{(3)} = 1)$ if the i-th and l-th oscillators are connected, otherwise $c_{i,l}^{(1)} = 0$ and $(c_{i,l}^{(2)} = 0, c_{i,l}^{(3)} = 0)$. The coupled oscillators (3), (4) have a homogeneous steady state

$$[Z_1^*, \cdots, Z_8^*]^T = [0, \cdots, 0]^T. \quad (5)$$

3. Stability analysis

The dynamics around the steady state in Eq. (5) is given by

$$\begin{aligned}\dot{z}_i(t) = (\mu + j\omega - 3k)z_i(t) \quad &+ \quad k\sum_{l=1}^{8} c_{i,l}^{(1)} z_l(t-\tau_1) \\ &+ \quad k\sum_{l=1}^{8} c_{i,l}^{(2)} z_l(t-\tau_2) \\ &+ \quad k\sum_{l=1}^{8} c_{i,l}^{(3)} z_l(t-\tau_3),\end{aligned} \quad (6)$$

where $z_i(t) := Z_i(t) - Z_i^*$ is a perturbation from the equilibrium point. The linear system in Eq. (6) can be rewritten as

$$\begin{aligned}\dot{\boldsymbol{X}}(t) = (\mu + j\omega - 3k)\boldsymbol{X}\,(t) &+ k(\boldsymbol{A}_G \otimes \boldsymbol{I}_4)\boldsymbol{X}(t-\tau_1) \\ &+ k(\boldsymbol{I}_2 \otimes \boldsymbol{A}_G \otimes \boldsymbol{I}_2)\boldsymbol{X}(t-\tau_2) \\ &+ k(\boldsymbol{I}_4 \otimes \boldsymbol{A}_G)\boldsymbol{X}(t-\tau_3),\end{aligned} \quad (7)$$

where $\boldsymbol{X}(t) := [z_1(t), \cdots, z_8(t)]^T$. The stability of the linear system in Eq. (7) is determined by the roots of the following characteristic equation,

$$\begin{aligned}G(s) = \det[(s - \mu - j\omega + 3k)\boldsymbol{I}_8 &- k(\boldsymbol{A}_G \otimes \boldsymbol{I}_4)e^{-s\tau_1} \\ &- k(\boldsymbol{I}_2 \otimes \boldsymbol{A}_G \otimes \boldsymbol{I}_2)e^{-s\tau_2} \\ &- k(\boldsymbol{I}_4 \otimes \boldsymbol{A}_G)e^{-s\tau_3}].\end{aligned} \quad (8)$$

As matrix $\boldsymbol{A}_G$ is a real symmetric matrix, it can be diagonalized as follows:

$$\boldsymbol{T}^{-1}\boldsymbol{A}_G\boldsymbol{T} = \begin{bmatrix}1 & 0 \\ 0 & -1\end{bmatrix} = \mathrm{diag}(1, -1), \quad (9)$$

where $\boldsymbol{T}$ is a transformation matrix. Thus, characteristic Eq. (8) can be diagonalized by using the transformation matrix $(\boldsymbol{T} \otimes \boldsymbol{T} \otimes \boldsymbol{T})$ as follows:

$$\begin{aligned}G(s) = \det[(\boldsymbol{T}^{-1} \otimes \boldsymbol{T}^{-1} \otimes \boldsymbol{T}^{-1}) \\ \{(s - \mu - j\omega + 3k)\boldsymbol{I}_8 - k\{(\boldsymbol{A}_G \otimes \boldsymbol{I}_4)e^{-s\tau_1} \\ + (\boldsymbol{I}_2 \otimes \boldsymbol{A}_G \otimes \boldsymbol{I}_2)e^{-s\tau_2} \\ + (\boldsymbol{I}_4 \otimes \boldsymbol{A}_G)e^{-s\tau_3}\}\} \\ (\boldsymbol{T} \otimes \boldsymbol{T} \otimes \boldsymbol{T})]\end{aligned}$$

$$
\begin{aligned}
&= \det[(s-\mu-j\omega+3k)\boldsymbol{I}_8 \\
&\qquad - k\{(\mathrm{diag}(1,-1)\otimes \boldsymbol{I}_4)e^{-s\tau_1} \\
&\qquad + (\boldsymbol{I}_2 \otimes \mathrm{diag}(1,-1)\otimes \boldsymbol{I}_2)e^{-s\tau_2} \\
&\qquad + (\boldsymbol{I}_4 \otimes \mathrm{diag}(1,-1))e^{-s\tau_3}\}].
\end{aligned} \tag{10}
$$

Consequently, characteristic Eq. (10) can be divided into eight modes,

$$
G(s) = \prod_{p=1}^{2}\left[\prod_{q=1}^{2}\left\{\prod_{r=1}^{2} g(s,\rho_p,\sigma_q,\phi_r)\right\}\right],
$$

$$
\begin{aligned}
g(s,\rho,\sigma,\phi) := s-\mu-j\omega+3k \\
- k(\rho e^{-s\tau_1}+\sigma e^{-s\tau_2}+\phi e^{-s\tau_3}),
\end{aligned} \tag{11}
$$

where $\rho_1=\sigma_1=\phi_1=1$ and $\rho_2=\sigma_2=\phi_2=-1$. The steady state in Eq. (5) is stable if and only if all the roots of eight modes in Eq. (11) stay on the left-half of the complex plane.

To determine the marginal stability curves and the stability region, we consider a root on the imaginary axis (i.e., $s=j\lambda$, $\lambda\in\mathbb{R}$). Substituting $s=j\lambda$ into $g(s,\rho,\sigma,\phi)=0$, we can obtain its real and imaginary parts:

$$
\begin{aligned}
-\mu+3k-k\{\rho\cos(\lambda\tau_1)+\sigma\cos(\lambda\tau_2)+\phi\cos(\lambda\tau_3)\}=0, \\
\lambda-\omega+k\{\rho\sin(\lambda\tau_1)+\sigma\sin(\lambda\tau_2)+\phi\sin(\lambda\tau_3)\}=0.
\end{aligned} \tag{12}
$$

The marginal stability curves on the (τ_1,τ_2) space are calculated employing the following numerical procedures [11]: set values for τ_1 and τ_3, solve Eq. (12) with respect to τ_2 and λ numerically[2], change the value of τ_1, and return to the first step.

4. Numerical example

Let us draw the marginal stability curves and the stability region on the connection parameter (τ_1,τ_2) space. The parameters of the oscillators are fixed at

$$
\mu=0.5,\ \omega=2\pi, \tag{13}
$$

and the coupling strength is set to $k=1.5$ [16].

Figure 2 shows the marginal stability curves (black curves) and the stability regions (gray areas) for $\tau_3=0, 0.5, 1.0, 1.5$. The marginal stability curves are the solutions for $g(j\lambda,\rho,\sigma,\phi)=0$ (i.e., Eq. (12)), on which at least one root of $g(s,\rho,\sigma,\phi)=0$ stays on the imaginary axis. Thus, if a parameter set (τ_1,τ_2) crosses the marginal stability curve, one root of $g(s,\rho,\sigma,\phi)=0$ crosses the imaginary axis. In the stability region, all roots of $g(s,\rho,\sigma,\phi,)=0$ stay on the left-half of the complex plane, while in the white areas, at least one root stays on the right-half of the complex plane.

[2]In the present study, we use fsolve in MATLAB for numerical calculation.

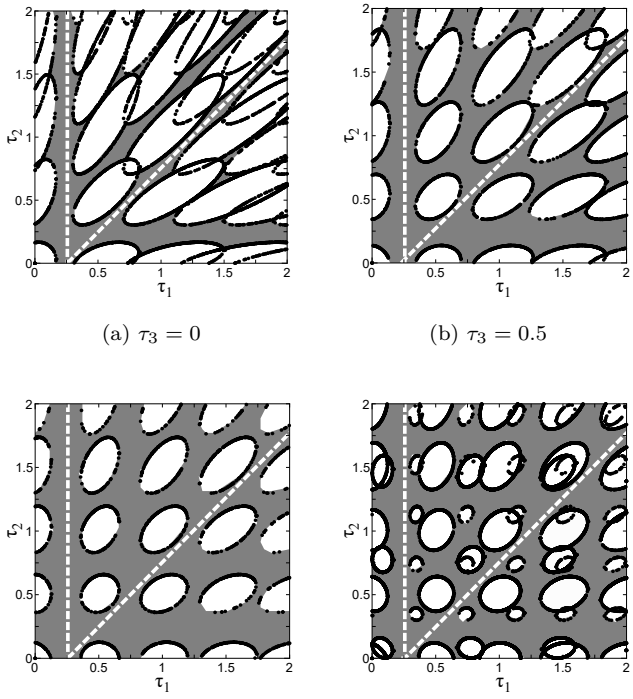

(a) $\tau_3=0$ (b) $\tau_3=0.5$

(c) $\tau_3=1.0$ (d) $\tau_3=1.5$

Figure 2: Stability region on the connection parameter (τ_1,τ_2). Black curves and the gray areas indicate the marginal stability curves and the stability regions for Cartesian product network $(\mathcal{G}_1\square\mathcal{G}_2)\square\mathcal{G}_3$, respectively, illustrated in Fig. 1 ($\mu=0.5, \omega=2\pi$).

It can be seen that the stability region strongly depends on the connection delay τ_3, for instance, Fig. 2(a) has a narrow region, while Fig. 2(c) has a wide region. However, regardless of the different connection delays τ_3, all stability regions in Figs. 2(a)-(d) contain two common white dotted lines: a vertical and a diagonal line. The vertical dotted lines imply that amplitude death can be induced for arbitrarily long τ_2 and τ_3 if τ_1 is fixed at an appropriate value (i.e., $\tau_1=0.25$). The diagonal dotted lines imply that amplitude death can be induced for arbitrarily long τ_3 if there is an appropriate difference between τ_1 and τ_2 (i.e., $\tau_2=\tau_1-0.25$). Stability regions on the (τ_1,τ_2) space were checked with $\tau_3=0, 0.5, 1.0, 1.5, 2.0, 5.0, 10$ and we have confirmed that the white dotted line is commonly observed for all τ_3. It should be noticed that a long connection delay never induce amplitude death if the connection delays are identical in the whole network (i.e., $\tau_1=\tau_2=\tau_3$) [5]. These results

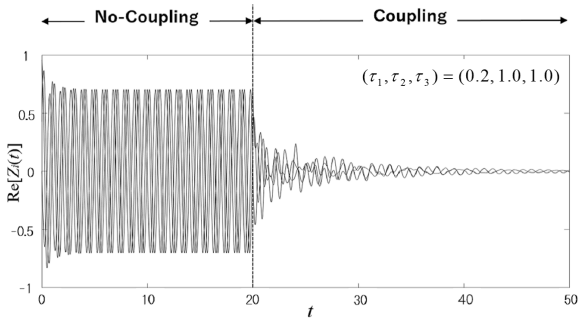

(a) point A: $(\tau_1, \tau_2) = (0.2, 1.0)$

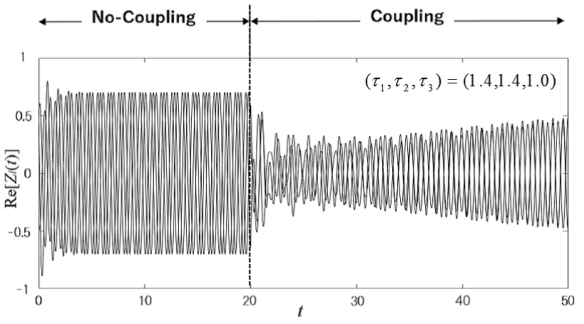

(b) point B: $(\tau_1, \tau_2) = (1.4, 1.4)$

Figure 3: Time-series date at points A and B in Fig. 2(c)

.

imply that there is a suitable difference between coupling delays in the sub-networks to induce amplitude death for long coupling delays.

Figure 3 shows the time-series date of the state variables $\mathrm{Re}[Z_i(t)]$ at points A: $(\tau_1, \tau_2) = (0.2, 1.0)$ and B: $(\tau_1, \tau_2) = (1.4, 1.4)$ in Fig. 2(c). All the oscillators are independent until $t = 20$. At $t = 20$, they become coupled. At point A, after coupling, all the variables converge to the equilibrium point (amplitude death). At point B, the variables still oscillate.

5. Conclusion

This study investigated amplitude death in a delayed coupled oscillator network on a cubic graph. Although the oscillator network had three different delays, the property of Cartesian product allowed us to simply determine the stability region. Our analytical results were confirmed by numerical simulations.

Acknowledgments

The present research was partially supported by JSPS KAKENHI (17K12748).

References

[1] A. Koseska *et al.*, Phys. Rep., vol. 531, pp. 173-199, 2013.

[2] G. Saxena *et al.*, Phys. Rep., vol. 521, pp. 205-228, 2012.

[3] Y. Yamaguchi and H. Shimizu, Physica D, vol. 11, pp. 212-226, 1984.

[4] D.G. Aronson *et al.*, Physica D, vol. 41, pp. 403-449, 1990.

[5] D.R. Reddy *et al.*, Phys. Rev. Lett., vol. 80, pp. 5109-5112, 1998.

[6] D.R. Reddy *et al.*, Physica D, vol. 129, pp. 15-34, 1999.

[7] S. Strogatz, Nature, vol. 394, pp. 316-317, 1998.

[8] S. Huddy and J. Skufca, IEEE Trans. Power Electron., vol. 28, pp. 247-253, 2013.

[9] F.M. Atay, Phys. Rev. Lett., vol. 91, p. 094101, 2003.

[10] Y. Kyrychko *et al.*, Eur. Phys. J. B, vol. 84 pp. 307-315, 2011.

[11] K. Konishi *et al.*, Phys. Rev. E, vol. 81, p. 016201, 2010.

[12] K. Konishi *et al.*, Phys. Lett. A, vol. 374, pp. 733-738, 2010.

[13] G. Saxena *et al.*, Phys. Rev. E, vol. 82, p. 017201, 2010.

[14] W. Zou *et al.*, Phys. Rev. E, vol. 86, p. 036210, 2012.

[15] W. Zou *et al.*, Phys. Rev. E, vol. 88, p. 032916, 2013.

[16] Y. Sugitani, Proc. NOLTA, pp. 667-670, 2016.

[17] M. Asllani *et al.*, Scientific Reports, vol. 5, 2015.

[18] F.M Atay and T. Biyikoglu, Phys. Rev. E, vol. 72, p. 016217, 2005.